Application of Artificial Neural Networks for Defect Detection in Ceramic Materials

Tahir Cetin AKINCI[1], H. Selcuk NOGAY[1], Ozgur YILMAZ[2]

[1] *Department of Electrical & Electronics Engineering*
Faculty of Engineering, Kirklareli University
Kirklareli-Turkey; e-mail: cetinakinci@hotmail.com, selcuknogay@kirklareli.edu.tr

[2] *Department of Computer Education & Instructional Technology*
Hasan Ali ucel Education Faculty, Istanbul University
Fatih, Istanbul-Turkey; e-mail: oyilmaz@istanbul.edu.tr

In this study, an artificial neural network application was performed to tell if 18 plates of the same material in different shapes and sizes were cracked or not. The cracks in the cracked plates were of different depth and sizes and were non-identical deformations. This ANN model was developed to detect whether the plates under test are cracked or not, when four plates have been selected randomly from among a total of 18 ones. The ANN model used in the study is a model uniquely tailored for this study, but it can be applied to all systems by changing the weight values and without changing the architecture of the model. The developed model was tested using experimental data conducted with 18 plates and the results obtained mainly correspond to this particular case. But the algorithm can be easily generalized for an arbitrary number of items.

Keywords: impulse noise, ANN, defect detection, ceramic materials.

1. Introduction

The use of ceramic materials is an indispensable part of our daily lives, occurring both as a part of artistic forms and a part of industrial processes (Bayazit, Bayazit, 2010). Ceramics are obtained by mixing inorganic industrial raw materials in certain ratios, shaping the end product, and hardening it by cooking. They are among the oldest tools used by mankind (Kucuk, Akinci, 2006) and were used since ancient times, especially for the production of kitchen utensils and the production of them still form the greatest production sector pertaining to ceramics (Bayazit, Bayazit, 2010).

Today, the ceramics industry forms the basis of many other industrial areas (Kucuk, Akinci, 2006). Ceramic materials are preferred for their certain advantages, such as resistance to high temperatures, lightness compared to metal materials, abundance of raw material sources, and resistance to wear, low coefficients of friction and high resistance. In recent years, special ceramics have found application fields in areas like computers, electronics and space research (Sawitz, 1999a; 1999b; Kubik, 2006; Uludag, 1998; SMPISTC, 2001).

The brittle nature of ceramic materials is their most important disadvantage. Since the compositions of ceramic materials contain metal oxides, silicates, carbides, nitrides, borides, glass etc, which can all be found in nature in abundance, their crystalline structures are very complex (MEGEP, 2007; Kamilov *et al.*, 1998). Amorphous structures or amorphous/crystalline joint structures may also be formed (Popovskaya, Bobkova, 2002; Samborski, Sadowski, 2005). Their material properties are based on their bond structures. They generally have low satiety and ductility, are hard and brittle. Sine they don't contain free electrons, they isolate electricity and heat well (Revel, Rocchi, 2006; De Andrade *et al.*, 1998; 1999). Because of the structure of their atomic bonds, they are chemically stable and have high melting points. The abundance in raw materials, the ease of their processing, the simplicity of their production, their low costs, the ease of their use, their hardness and resistance to heat increase their fields of use. Beside these, the most important problem in ceramic materi-

als is the brittleness and deformation property of those materials. The greatest disadvantages of ceramics and porcelains used in industry and as kitchen utensils are breaking and cracking.

Mechanical failure in ceramic materials mostly stem from structural imperfections. These structural imperfections are surface cracks, pores, residues and large particles that are formed during production (DE ANDRADE *et al.*, 1998; 1999; RANACHOWSKI, REJMUND, 2008).

All ceramic materials are brittle. Their observed tensile strength is about 0.70 MPa. In some special ceramics, a value of 7000 MPa can be reached through A12O3 fibers. The impact resistances of hard ceramics are low because of their ionic collective bonds (SMP-ISTC, 2001; ULUDAG, 1998; MEGEP, 2007).

In some ceramics, through stacking or storing mistakes, grain boundaries with small angles or twin grain boundaries may be form. However, the surfaces of ceramic particles are much more important since their breaking surface may be exposed (ULUDAG, 1998). Since these break and cracks are not visible in enamelled ceramics, such deformations have to be detected through special methods. In this study, the cracks formed in ceramic pales were detected through impact noise. To obtain impact noise, it is necessary to apply a fixed impact A pendulum was used for this purpose.

The impulse noise generated by the measuring system was then digitized and transferred to the signal processing unit (a personal computer PC) as the input data fort it developed the ANN algorithm. Pendulums have a quite interesting dynamic system. They are such physical devices that make angular movements and cause the same effects by forming the same movements (RANACHOWSKI, REJMUND, 2008; BEVIVINO, 2009; KATER, 1996).

Using Fig. 1 one can begin deriving the equation of motion for the pendulum. Equation (1) becomes, by use of

$$\mathbf{\Gamma} = \mathbf{r} \times \mathbf{F}, \tag{1}$$

$$-\text{damping}_{\text{force}} = \text{gravity}_{\text{force}} + \text{driving}_{\text{force}} = I\ddot{\theta}, \tag{2}$$

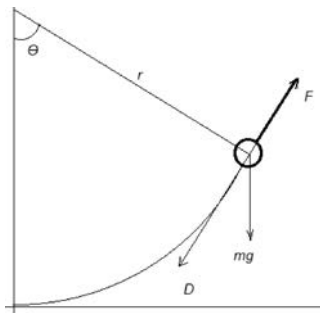$$-bvr\sin\theta + -mgr\sin\theta + Fr\sin\theta = I\ddot{\theta}. \tag{3}$$

Fig. 1. Scheme of a pendulum (AKINCI, 2011).

Let the damping and driving forces be parallel to the motion of the pendulum. Let the driving force be a function of time. Let $D = bv$, so the damping force is dependent on the velocity, v or $r\dot{\theta}$. Rearranging and substituting gives:

$$mr^2\ddot{\theta} + br^2\dot{\theta} + mrg\sin\theta = F(t)r, \tag{4}$$

$$\ddot{\theta} + \frac{b}{m}\dot{\theta} + \frac{g}{r}\sin\theta = \frac{F(t)}{mr}. \tag{5}$$

Equation (5) is a second order differential equation describing the dynamical system of interest (BEVIVINO, 2009; KATER, 2008; AKINCI, 2011). The paper is organized as follows. In the next section a brief introduction to the ANN algorithm is given. In Sec. 3, the experimental setup is shown and in Sec. 4, the selected parameters of the developed ANN are explained. In Secs. 5 and 6, the training and testing ANN are briefly commented, respectively. And finally, a discussion of the obtained results is given in Sec. 7.

2. Artificial Neural Network (ANN)

Artificial Neural Networks (ANN) are complex computational or mathematical models developed in order to process information in the way inspired by the nature of biological neural networks. They are usually adaptive systems for non-linear data processing, used intensively for modelling complex relations between inputs and outputs, pattern recognition, etc.

There are many of different types of ANN models. The most popular of them include the multilayer perceptron, which is generally trained with the back propagation algorithm. In Fig. 1 two layers feed forward network for general application of ANN is illustrated. Back propagation is a training method for multilayer feed forward networks. Such an ANN model network proposed for this study, including three layers of perceptrons is shown in Fig. 2. In this study, thirty-five number of neuron was used in the hidden layer, sixteen input parameters and five output parameters were used in the input layer as shown in Tables 1 and 2, respectively (HAGAN *et al.*, 1996; AKINCI, 2011; BOX, JENKINS, 1970).
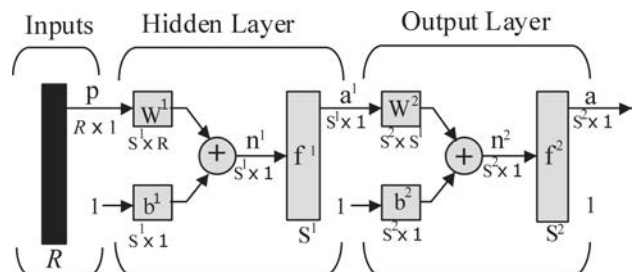

Fig. 2. Two-layer feed forward network.

By the algorithmic approach known as the Levenberg-Marquardt back propagation algorithm,

the error is decreased repeatedly. Some ANN models employ supervisory training while others are referred to as none-supervisory or self-organizing training. However, the vast majority of ANN models use supervisory training (Fig. 3). The training phase may consume a lot of time. In the supervisory training, the actual output of ANN is compared with the desired output. The training set consists of presenting input and output data to the network. The network adjusts the weighting coefficients, which usually begin with a random set, so that the next iteration will produce a closer match between the desired and the actual output. The training method tries to minimize the current errors for all the processing elements. This global error reduction is created over time by continuously modifying the weighting coefficients until the ANN reaches the user defined performance level. This level signifies that the network has achieved the desired statistical accuracy for a given sequence of inputs. When no further training is necessary, the weighting coefficients are frozen for the application. After a supervisory network performs well on the training data, then it is important to see what can it do with data which it had not seen before. If a system does not give reasonable outputs for this test set, the training period is not over. Indeed, this testing is critical to insure that the network has not simply memorized a given set of data, but has learned the general patterns involved within the application (HAGAN *et al.*, 1996; AKINCI, 2011; BOX, JENKINS, 1970).
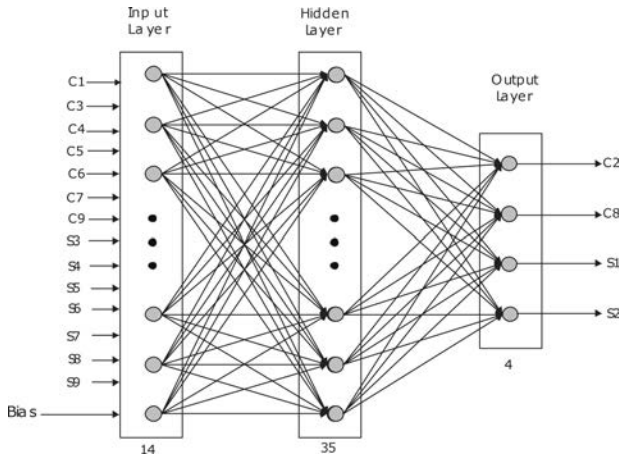

Fig. 3. Proposed ANN model.

The back-propagation learning algorithm is presented below in brief. For each neuron in the input layer, the neuron outputs are given by

$$n_i = o_i, \qquad (6)$$

where n_i is the input of neuron i, and o_i the output of this neuron. Again for each neuron in the output layer, the neuron inputs are given by

$$n_k = \sum_{j=1}^{N_j} w_{kj} o_j, \qquad k = 1, 2, 3, ..., N_k, \qquad (7)$$

where w_{kj} is the connection weight between neuron j and neuron k, and N_j, N_k the number of neurons in the hidden layer and output layer, respectively. The neuron outputs are given by

$$o_k = \frac{1}{1 + \exp\left[-\left(n_k + \theta_k\right)\right]} = f_k\left(n_k, \theta_k\right), \qquad (8)$$

where θ_k is the threshold of neuron k, and the activation function f_k is a sigmoidal function. For the neurons in the hidden layer, the inputs and outputs are given by relationships similar to those given in Eqs. (2) and (3), respectively.

The connection weights of the feed-forward network are derived from the input–output patterns in the training set by the application of the generalized delta rule. The algorithm is based on minimization of the error function on each pattern p by the use of the steepest descent method. The sum of squared errors E_p that is the error function for each pattern is given by

$$E_P = \frac{1}{2} \sum_{k=1}^{N_k} (t_{pk} - o_{pk})^2, \qquad (9)$$

where t_{pk} is the target output for the output neuron k, and o_{pk} is the calculated output for the output neuron k. The overall measure of the error for all the input-output patterns is given by

$$E = \sum_{p=1}^{N_p} E_p, \qquad (10)$$

where N_p is the number of input-output patterns in the training set. When an input pattern p with the target output vector t_p is presented, the connection weights are updated by using the following equations:

$$\Delta w_{kj} = \eta \delta_{pk} o_{pj} + \alpha \Delta w_{kj}(p-1), \qquad (11)$$

$$\delta_{pk} = (t_{pk} - o_{pk}) o_{pk}(1 - o_{pk}), \qquad (12)$$

where η is the learning rate, and α is the momentum constant. Again, the connection weights between input the layer neuron i and the hidden layer neuron j can be updated by using the following equations:

$$\Delta w_{ji} = \eta \delta_{pk} o_{pj} + \alpha \Delta w_{ji}(p-1), \qquad (13)$$

$$\delta_{pj} = o_{pj}(1 - o_{pj}) \sum_{k=1}^{N_k} \delta_{pk} w_{kj}. \qquad (14)$$

It is important to note that the threshold θ of each neuron is learned in the same way as that for the other weights. The threshold of a neuron is regarded as a modifiable connection weight between that neuron and a fictitious neuron in the previous layer which always has an output value of unity (HAGAN *et al.*, 1996; AYDOGMUS, 2009; BOSE, 2002).

In order to use the ANN simulator for any application, the number of neurons in the layers, type of activation function (purelin, tansig, logsig), the number of patterns, and the training rate must first be chosen.

The ANN designing process involves five steps. These are gathering the input data, normalizing the data, selecting the ANN architecture, training the network, and validation-testing the network.

3. The measurement system and data acquisation

In this study, a pendulum was used to produce a stable impulse. The Impact Pendulum is an improved pendulum model used for creating equal magnitudes of impacts (KAMILOV *et al.*, 1998). Through a little plastic hammer attached to the end of the Impact Pendulum it was provided to have equal magnitudes of impact hits without any damages to the ceramic plate and it was intended to analyse the sound coming from the plate. The measurement and data acquisition can be represented as shown in Fig. 4.
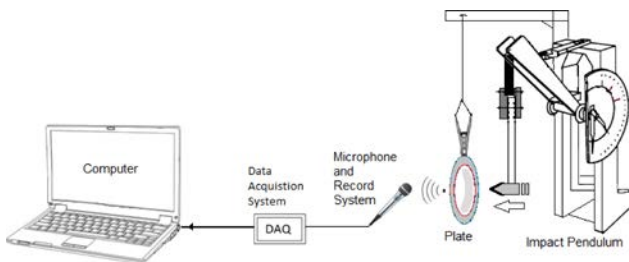

Fig. 4. Data acquisition and measurement systems (AKINCI, 2011).

In the study, the POE 2000 type Impact Pendulum was used and the effect to hit the ceramic plate with the same magnitude was achieved. Here, using the Impact Pendulum, the sound coming out as a result of applying equal impacts on the same type and model of plates with or without cracks (in good condition) was transferred to the data collection system, then from the data collection system to the computer and the data processing stage was started. In this study, the sound system model Onyx 800R is used. The output audio data of the amplifier is transmitted to the computer at a sampling rate of 0.0000125 seconds via the Advantech 1716L Multifunction PCI card and the data analysis is performed using Matlab (Fig. 5).

Ten ceramic plates, including those in good condition and those that have different cracks, were determined and plates with impacts of equal magnitudes were applied. The differences of the sounds from the ceramic plates in the same impact are shown in Fig. 5.

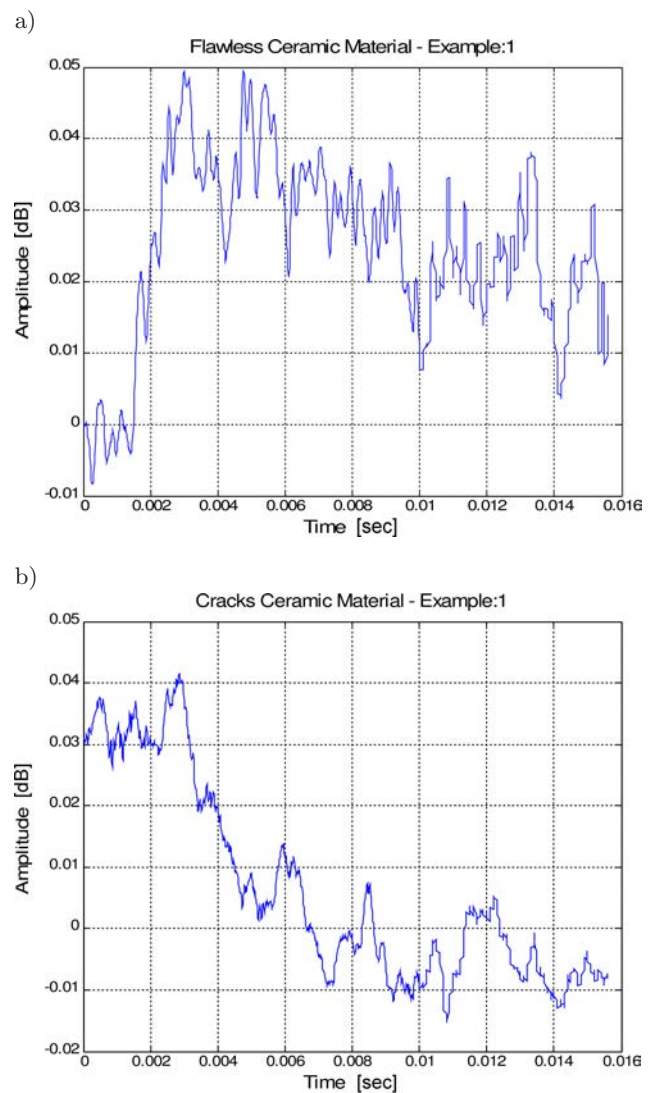The assessments of the time-amplitude graphics of the cracked and good plates are given in Fig. 5. Ac-

a)

b)

Fig. 5. Noise plot of undamaged and cracked plates (AKINCI, 2011): a) undamaged plate, b) cracked plate.

cording to this graphic, there is a sound absorption through the crack openings in the cracked plate after the impact and the vibration does not continue; on the contrary, the vibration in the plate in good condition continues for a longer period on the same level. This situation shows a similar trend in other graphics though it changes according to the size and shape of the cracks in the plates. Here, only one of the five tests was examined. The cracked plates made of different material were used in each experiment.

A summary of the data set used in the study is presented in Table 1. It is also possible to see the input and output data, and the maximum and minimum values for intact and cracked plates in this table. In the study, intact plates were named with "*s*" and the cracked ones were named with "*c*". The numbers following the letters (*s* or *c*) denote the plate numbers.

Before further processing the measured data were normalized for convenience.

Table 1. Data Set Summary.

	Maximum value	Minimum value	Symbol
Input	0.0415	−0.0153	c1
	0.0128	−0.0358	c3
	0.0214	−0.0351	c4
	0.0315	−0.0159	c5
	0.0345	−0.0429	c6
	0.5260	−0.1970	c7
	0.0338	−0.0053	c9
	0.0447	−0.0180	s3
	0.0560	−0.0094	s4
	0.0440	−0.0202	s5
	0.0314	−0.0167	s6
	0.0400	−0.0344	s7
	0.0380	−0.0507	s8
	0.0437	−0.0139	s9
Output	0.0063	−0.0318	c2
	0.0495	−0.0084	s1
	0.0349	−0.0196	c8
	0.0379	−0.0103	s2

4. Selecting the ANN architecture

The number of layers and the number of processing elements per layer are important decisions for selecting the ANN architecture. Choosing these parameters to a feed forward back propagation topology is the art of the ANN designer. There is no quantifiable best answer to the layout of the network for any particular application. There are only general rules picked up over time and followed by most researchers and engineers applying this architecture to their problems. The first rule states that if the complexity in the relationship between the input data and the desired output increases, then the number of the processing elements in the hidden layer should also increase. The second rule says that if the process being modelled is separable into multiple stages, then additional hidden layer(s) may be required. The result of the tests has showed that the optimal number of neurons in the hidden layer can be chosen as 35 and the activation function has been chosen as a hyperbolic tangent sigmoid function for all the layers.

5. Training the network

In this study ANN was trained with the back propagation (Levenberg-Marquardt) training algorithm. In the training process of this study, the actual output of ANN was compared with the desired output. The training set consists of fourteen input and four output data to the ANN model. The number of data was 1024; 90% of this data were used for training. The network adjusted the weighting coefficients that began

with the random set. The training process has been stopped when the error has become stable. The ANN simulator has been trained through the 61 epochs as shown in Fig. 6.
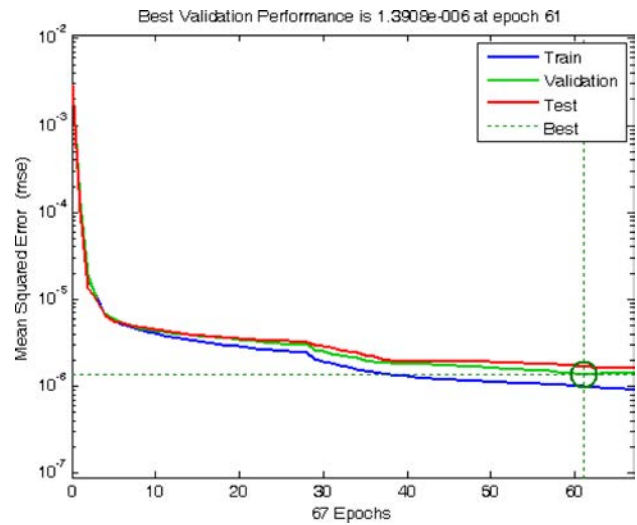

Fig. 6. Training process of the developed ANN algorithm.

6. Testing the network

In the test, an unknown input pattern has been presented to the ANN, and the output has been calculated. A linear regression between the ANN output and target is performed. After the ANN test in step, founded regression coefficients for C2, C8, S1 and S2 outputs ($R = 0.98389$, $R = 0.99348$, $R = 0.99286$ and $R = 0.99669$, respectively) reveals a good agreement between the target and ANN output values. The results of regression analyses are shown in Fig. 7. These coefficient shows that the target and ANN output values were very related to each other.
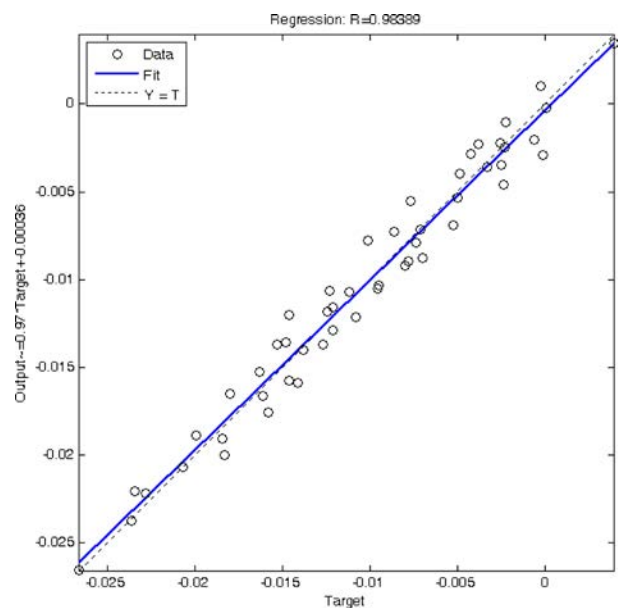

Fig. 7. Regression results of the system for C2.

7. Results and discussions

There are many different statistical methods in the literature. The most common methods mean absolute error (MAE), mean squared error (MSE), root mean squared error (RMSE), and mean absolute percentage error (MAPE). Those were used in this study as seen in Table 2.

With the ANN prediction model developed, the intactness of any four of the 18 plates, of which 9 was cracked, was predicted. Since the prediction was performed basing on the sound data at hand, the details of the deformations can be interpreted by checking the depth of the crack. In the study, only the conditions of the plates with the code numbers C2 and C8 from among the cracked plates and S1 and S2 from among the intact plates were predicted. After all, the real goal of this study is not finding cracked plates but examining the cracks or determining the properties of the cracks. For this purpose, the impact noises that all plates produced as a result of the test conducted through the pendulum were recorded. The goal is to make a right prediction. When Table 2 is examined, it can be clearly seen how low are the values denominating the error. The regression values for every output are proofs of the success of the prediction model. For example, the output of S2 from Table 2 was predicted with a correctness of 99.6%. This means that, through the predicted curve of the S2 plate, an idea can be obtained about how intact is this plate compared to other plates besides identifying the plate as cracked.

Since four outputs were used in the system, it is possible to obtain separate curves for each output. A three-dimensional chart showing all outputs at once can be seen in Figs. 8a and 8b. Even though these three-dimensional charts obtained only from test data look the same, there are error differences between them, albeit small ones. For example, when we look at the last curve of the first output curve line in both of the curves, we can see that the last data indicate a falling trend in the target chart, whereas they are slightly vertex in the output chart.

When separate curves are drawn for every output, they are as shown in Figs. 9–12. Among them Fig. 9 is a chart comparing the true value to the predicted one obtained only for the C2 output.

The proximity of the two curves in Fig. 10 shows the success of the system. The system determines the crack level or intactness of the plate according to the similarity between the true chart and the predicted one. In other words, when one looks as in Fig. 10, where the crack curve of the plate with code number C2 is the target curve that corresponds to the prediction curve of the system, one can say that the plate with the code number C2 is deformed or cracked.

In Fig. 10, the intactness curve of the plate with code number S1 was used. Here, similarly to Fig. 9, the intactness curve of the plate was used to check whether the plate was intact. When the output of the ANN prediction model is compared to the intactness curve in Fig. 10, their proximity can be easily seen. In that case, it can be said that the plate with the code number S1 is intact.

Table 2. Performance of the system.

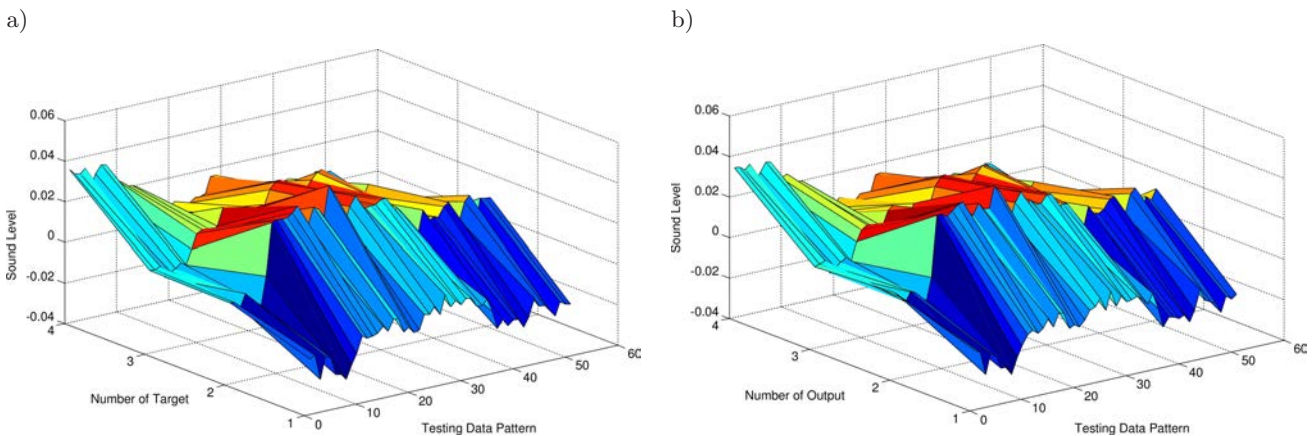| Output	MAPE	MAE	MSE	RMSE	R
C2	0.227133323	0.001073978	0.00000161381	0.00127035	0.98389
C8	0.154625299	0.000962429	0.00000151338	0.00123019	0.99348
S1	0.159036303	0.001305272	0.00000258198	0.00160685	0.99286
S2	1.705792685	0.00082323	0.00000102769	0.00101375	0.99669

a)

b)

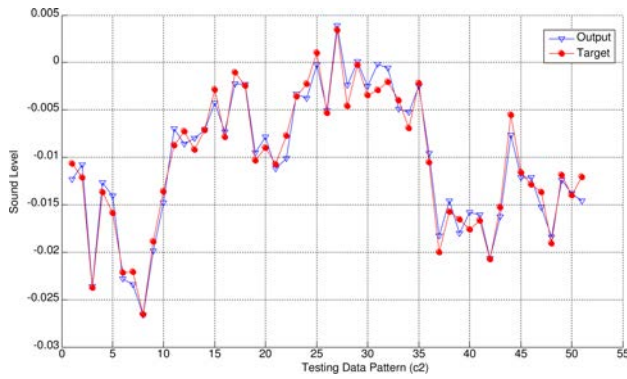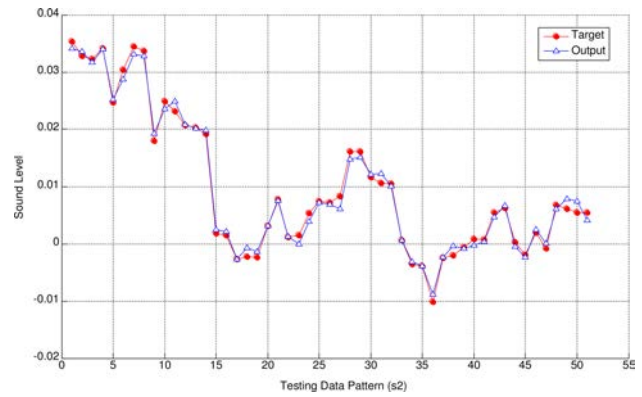Fig. 8. Variation of the ANN testing data (a) output, (b) target.

Fig. 9. Comparison of the testing data
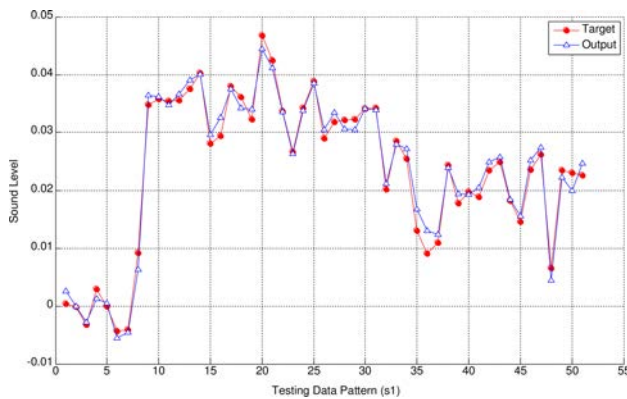with the target ones.

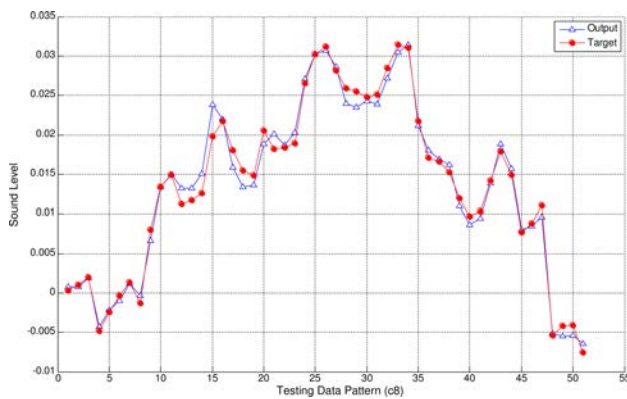Fig. 10. Comparison of the testing data
with the target ones.

Fig. 11. Comparison of the testing data
with the target ones.

Comparison of the testing data with the target ones are shown Fig. 11. In Fig. 12, just like in Fig. 10, the intactness curve of the plate with code number S2 was compared to the output of the ANN and the intactness of the plate was confirmed. In order to determine the wear conditions of the plates, the intactness and crack data from the plates of the same kind are needed. With those curves, it is possible to obtain prediction models and data sets that allow one to check the physical conditions of the plates and calculate the lifespan of them.

Fig. 12. Comparison of the testing data
with the target ones.

8. Conclusions

In this study, a multi-layered artificial neural network model was developed in order to determine the deformation condition (whether cracked or not) of a ceramic material. Experimental applications were performed in order to obtain a data set that would be used in the ANN model. As a result of these experiments, the data set to be used in the training and testing of the ANN model was trained with the impact noises of impacts applied on 18 ceramic plates, 9 of which were cracked

The following results have been obtained:

- The deformation level of a ceramic material was measured.
- A data set was formed from the data obtained according to different deformation conditions.
- A multi-layered ANN model was developed. Using 90% of the data set that was formed, the ANN model as trained with the Back propagation learning algorithm. With the other 10% of the data set, the success of the system was tested.
- At the end of the test, the deformation conditions of the cracked or intact plates were predicted with a success rate of 98.38% for the plate with code number C2, 99.34% for the plate with code number C8, 99.28% for the plate with code number S1, and 99.66% for the plate with code number S2.

As a result of the study, it was found that the experimental results for intact and cracked plates and the ANN outputs were very consistent with each other.

References

1. AKINCI T.C. (2011), *The Defect Detection in Ceramic Materials Based on Time-Frequency Analysis by Using the Method of Impulse Noise*, Archieves on Accoustic, **36**, 1, 77–85.

2. AYDOGMUS Z. (2009), *A neural network-based estimation of electric fields along high voltage insulators*, Expert Systems with Applications, **36**, 8705–8710.

3. BAYAZIT M., BAYAZIT E. (2010), *Evaluation of Ceramic Materials on Art*, Journal of Applied Sciences Research-INSInet Publication, **6**, 6, 790–795.

4. BEVIVINO J. (2009), *The Path From the Simple Pendulum to Chaos*, Dynamics at the Horsetooth, **1**, 1–24.

5. BOSE B.K. (2002), *Modern power electronics and AC drivers*, Prentice Hall PTR, USA, p. 625–689.

6. BOX G.E.P., JENKINS G. (1970), *Time Series Analysis, Forecasting and Control*, Golden-Day, San Francisco, CA.

7. Ceramics and Glass Technology, (2007), Republic of Turkey Ministry of National Education, [MEGEP], p. 340–355.

8. DE ANDRADE R.M., PAONE N., REVEL G.M. (1998), *Non Destructive Thermal Detection of Delamination in Ceramic Tile*, Proc. ENCIT 98, pp. 727–731, Rio de Janeiro.

9. DE ANDRADE R.M., ESPOSITO E., PAONE N., REVEL G.M. (1999), *Non-destructive Techniques for Detection of Delamination in Ceramic Tile: A Laboratory Comparison Between Ir Thermal Cameras and Laser Doppler Vibrometers*, Proc. SPIE, **3585**, 367–377.

10. HAGAN T.M., DEMUTH H.B., BEALE M. (1996), *Neural Network Design*, PWS Publishing Company, Boston, 2–44.

11. KAMILOV S., KARABAEVA M., ABDURRAHMANOV M. (1998), *Studies of Structure of Ceramic Materials Containing Molibdenum Particles Within the Framework of Theory of Non-Homogeneous Systems*, TUBITAK, Tr. J. of Physics, **22**, 777–781.

12. KATER H. (1818), *An account of experiments for determining the length of the pendulum vibrating seconds in the latitude of London*, Phil. Trans. R. Soc. (London), **104**, 33, 109, [Retrieved (2008)-11-25].

13. KUBIK J. (2006), *Durability of monuments* [in Polish: *Trwałość zabytków*], Studia z zakresu Fizyki Budowli. Sekcja Fizyki Budowli KILiW PAN, Łódź.

14. KUCUK H., AKINCI T.C. (2006), *Roughness of Ceramic Materials by the Method of Determining Noise Impact*, Conference For Computer Aided Engineering And System Modelling, Abant Palace Hotel, Bolu-Turkey.

15. MALDAGUE X.P.V. (2001), *Theory and Practice of Infrared Technology for Nondestructive Testing*, pp. 238–250, John Wiley & Sons, New York.

16. POPOVSKAYA N.F., BOBKOVA N.M. (2002), *Mullite-Tialite Ceramic Materials Based on Chemically Precipitated Mixtures (A Review)*, Glass and Ceramics, **59**, 7–8, 234–236, DOI: 10.1023/A:1020979228914.

17. RANACHOWSKI P., REJMUND F. (2008), *Mechanical-Acoustic Examination of Ceramic Material*, Proceedings of the 7th Int. Conference EEEIC 08, Cottbus, pp. 11–13.

18. REVEL G.M., ROCCHI S. (2006), *Defect detection in ceramic materials by quantitative infrared thermography*, 8th Conference on Quantitative Infrared Thermography – QIRT'2006, Padova, Italy.

19. SAMBORSKI S., SADOWSKI T. (2005), *Experimental Investigations and Modelling of Porous Ceramics, Solid Mechanics and ıts Applications*, IUTAM Symposium on Multiscale Modelling of Damage and Fracture Processes in Composite Materials Proceedings of the IUTAM Symposium held in Kazimierz Dolny, Poland.

20. SAWITZ M. (1999), *Commercialisation of Advanced Ceramics,* Part I, Am. Ceram. Soc. Bull., **78**, 1, 53–56.

21. SAWITZ M. (1999), *Commercialisation of Advanced Structural Ceramics*, Part II, Am. Ceram. Soc. Bull., **78**, 3, 52–56.

22. Stone and Mineral Products Industry Special Trade Commission Report [SMPISTC], (Ceramic Coating Materials, Ceramic Health Care Products, Technical Ceramics), DPT: 2552 – ÖÝK: 568, ISBN 975-19-2807-9, Ankara 2001 Turkey.

23. ULUDAG K. (1998), *Ceramic Art of Identity Problem*, Journal of Art in Turkey, **33**, 36–38.